

IAC-12-C4.2.11

VISUALIZATION OF THE LIQUID LAYER COMBUSTION OF PARAFFIN FUEL AT ELEVATED PRESSURES

Ashley A. Chandler

Stanford University, United States, achandlr@stanford.edu

Elizabeth T. Jens

Stanford University, United States, etjens@stanford.edu

Brian J. Cantwell

Stanford University, United States, cantwell@stanford.edu

G. Scott Hubbard

Stanford University, United States, scotthub@stanford.edu

High regression rate hybrid rockets (e.g. those using paraffin-based fuel) show great promise for a variety of applications including space tourism, solar system exploration and launch vehicles. However, the mechanism responsible for the increased regression rates enjoyed by these fuels over classical hybrid fuels is still not fully understood. Combustion of paraffin-based hybrid rocket fuel with gaseous oxygen has been observed at elevated pressures using a facility developed at Stanford University. These results are compared to previous atmospheric pressure runs and differences in the combustion with increasing pressure are discussed. Conditions between the two runs were kept as similar as possible to facilitate this comparison. The elevated pressure runs showed a marked difference in the combustion. The large number of droplets fed by roll waves in the unstable liquid layer predicted by the increased high regression theory were not evident in these runs. Instead, many filament-like structures are visible in the combustion process.

I. INTRODUCTION

I.1 Hybrid Rockets

Hybrid rockets typically consist of a solid fuel and liquid oxidizer. Combustion occurs in the gas phase. It is initiated when the liquid oxidizer is atomized or vaporized across an injector and mixes with fuel vapour created by the igniter. The combustion process is then self-sustaining. Classically, this process has been diffusion limited.

Hybrid rockets have historically had lower performance due to low fuel regression rates and therefore low mass transfer rates and thrust levels. This arises from the fact that the combustion process within conventional hybrid rockets relies on a relatively slow mechanism of heat transfer leading to fuel sublimation and diffusive mixing of the fuel and oxidizer. Conventional hybrid rockets overcome low thrust levels by increasing the fuel surface burning area through complex, multi-port fuel grains.

The classical, diffusion limited model splits the boundary layer into two zones, separated by an infinitely thin flame sheet. The region above the flame is oxidizer rich and the region below is fuel rich. The

flame occurs at the point where the oxidizer and fuel exist in a combustible concentration, but not necessarily at the stoichiometric mixture.¹ A sketch of the turbulent boundary layer, including the behavior of several important parameters, is included in Figure 1.

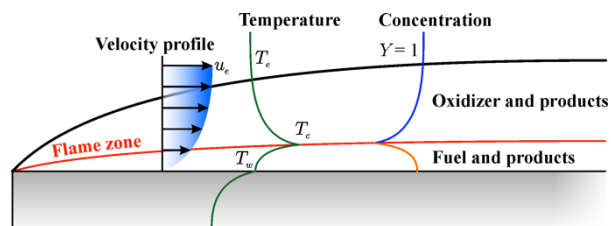


Fig. 1: Diffusion limited classical hybrid rocket combustion. Oxidizer flow is from left to right.

I.1 High Regression Rate Hybrid Fuels

High regression rate fuels have brought hybrid rockets to the forefront of propulsion research. These fuels form a thin melt layer during combustion, which is unstable under the oxidizer flow. It has been predicted that the shear force between the liquefied fuel and vaporized oxidizer creates roll waves in the liquid layer and forces droplets of fuel to separate and entrain into

the flow.³ This process is essentially a fuel injection system, which dramatically increases the mass transfer and therefore the regression rate of the fuel (by 3-4 times that of classical hybrid fuels.)

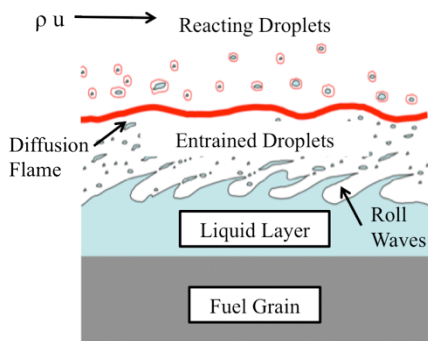


Fig. 2: Conceptual sketch of the entrainment mechanism predicted for high regression rate hybrid fuels. (Derived from Figure 6 in Cantwell et al.²) Oxidizer flow is from left to right.

The thrust levels required by most classical hybrid propulsion systems led to the need for increased burning areas in order to provide sufficient mass flux. This was often realized by complex, multi-port fuel grain designs that have been responsible for most of the disadvantages associated with hybrid rockets. The increased mass transfer of liquefying hybrid fuels enables simple, single-port fuel grain designs to make competitive candidates for a variety of launch systems and in-space missions. The mechanism responsible for the fast regression rates of liquefying fuels has been predicted theoretically,³ however, is still poorly understood.

II. EXPERIMENTAL SET UP

II.I Visualization Apparatus

An apparatus to visualize the liquid layer combustion of hybrid rocket fuels with gaseous oxygen has been designed and constructed at Stanford University. It is capable of oxidizer mass fluxes up to about 5 g/cm²s (50 kg/m²s) and pressures up to 1.7 MPa. The set up is shown in Figure 3.

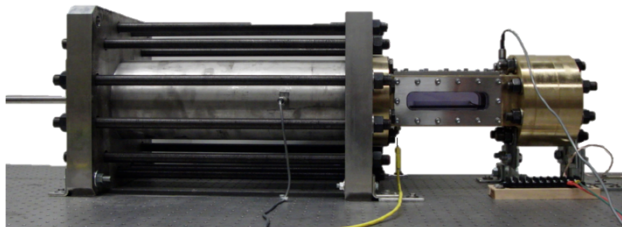


Fig. 3: The visualization apparatus. Flow is from left to right.

The inlet from the feed system is visible at the far left of Figure 3. The oxidizer then passes through the flow conditioning system and into the combustion

chamber. The two pressure transducers have grey wires and the yellow wiring leads to a thermocouple upstream of the fuel in the combustion chamber. The nozzle is inserted at the aft end of the combustion chamber, within the brass section at the far right.

The main components making up the apparatus are a flow conditioning system and combustion chamber. The flow conditioning system is used to create uniform and predictable oxidizer flow at the inlet of the combustion chamber. It was designed using rules for a low speed wind tunnel.⁴

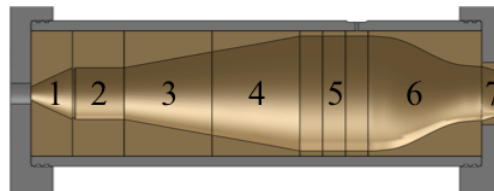


Fig. 4: The flow conditioning system modelled after a low speed wind tunnel. 1: Inlet; 2: Flow trip and reservoir; 3-4: Wide angle diffuser; 5: Three screen settling chamber; 6: Contraction; 7: Circle to square transition.

The combustion chamber was machined out of a single brass cylinder. The test section is 5 by 5 cm and has three windows that allow visual access to the combustion chamber as well as various lighting options.

The system can be run at various pressures by inserting or removing the nozzle. To date, 22 tests have been run at atmospheric pressure and 3 have been run at elevated pressures. Pressure measurements are taken at the aft end of the settling chamber in the flow conditioning system as well as at the end of the combustion chamber.

These tests are run using paraffin wax with black dye and gaseous oxygen. The black dye is used to minimize radiative heat penetration into the solid fuel grain. Wax without blackener is more susceptible to sloughing off without burning. The tests reported here utilized a copper fuel grain support. Some of the initial tests used an alternative material (G10 garolite), which adversely affected the flow near the end of the burn.

The test procedure begins by opening the main oxidizer valve. After a short delay, voltage is applied across a 26-gauge nichrome wire coated with epoxy to initiate combustion. It is quenched with gaseous nitrogen after the programmed time, which is input for each test. The test is controlled and data is acquired with a National Instruments LabView code.

II.I Cameras

The combustion is visualized using a Casio Exilim EX-F1, capable of 1200 frames per second (fps). At high speeds, the field-of-view of the camera decreases with increased frame rate. Instead of reducing the

resolution, the available area shrinks in to a long and slender rectangle at 1200 fps. The windows were designed to match this shape. More detail can be captured if the area being filmed is smaller. For this reason, a view of the entire window area along with a zoomed in view is included in the results.

III. EXPERIMENTAL RESULTS

Twenty-five hot fire tests have been conducted with this system to date. Three tests will be discussed to compare the effects of pressure on the combustion of high regression rate hybrid fuels. Two of these tests were conducted at atmospheric pressure and one at elevated pressure. The parameters for the tests can be found in Table 1. These include the date on which the test was conducted in day/month/year format, the average oxidizer mass flux rate, the approximate burn time, the burned mass and the oxidizer to fuel ratio. The camera settings are also included for reference.

	Atmospheric Pressure		Elevated
	Full	Zoom	Pressure
Test Date	23/5/'12	25/5/'12	11//8/'12
Avg. Oxidizer Mass Flux (g/cm ² s)	2.61	2.69	1.08
Approx. burn time (s)	3.5	3.4	~4
Burned mass (g)	6.0	5.1	13.2
Camera Settings	Frame Rate	1200	1200
	Fstop	4.6	4.6
	Shutter Speed	1/32,000	1/32,000
			1/32,000

Table 1: Parameters for the tests being compared. *The zoomed out camera was set to 4.4 and the zoomed in view was set to 4.6. Unlike the atmospheric pressure case, both views were capturing the same test.

The burned mass was calculated by carefully removing all remaining fuel after the run and subtracting its mass from the original mass of the fuel grain. There is some uncertainty associated with this method, since some of the fuel may not be recovered (e.g. it may be ejected unburned).

III.I Atmospheric Pressure Tests

Two tests are presented to describe the atmospheric pressure results. The details of these tests were reported in Chandler.⁵ Neither of these tests included a nozzle in order to maintain atmospheric pressure in the combustion chamber.

Full View Atmospheric Test

This test captured the full window area (approximately 17.8 cm by 3.8 cm) and gives an overall view of the combustion process, including some geometric effects (e.g. vortex flame rolling over the aft end of the fuel grain). The roll waves can barely be seen in this test, but are circled in blue in Figure 5. Large droplets above the flame sheet were visible through out the test.

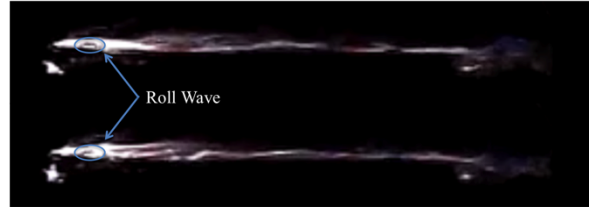


Fig. 5: Progression of a wave in the liquid layer during an atmospheric test. The raised ring in the top image breaks off in the bottom image.

The flame structure is thin and drawn out. It changes readily throughout the test as the flames move along the length of the grain. The thickness of the optically bright region of the flame is observed by combining images over the length of the burn. The composite image, shown in Figure 6, was created by combining frames and making them partially transparent, which allows the brightest features show through. The stills are roughly 300 frames apart (0.25 seconds) and are taken without analysis of the frame itself to get an unbiased view of the thickness. It should be noted that these calculations are very rough. The images are composites over the entire burn, during which the fuel surface is regressing. This discussion is only meant to give some scale to the images. The known height of the window is used to determine the scale. The maximum thickness of the optically bright region of the flame was almost 5 mm in this case.

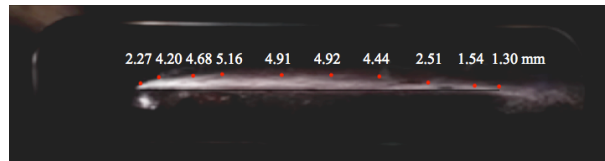


Fig. 6: Thickness of the optically bright region of the flame from the atmospheric pressure test. The height of the red dots above the black baseline is given in millimeters.

The droplets visible in this test were predominately above the level of the flame. They are also fairly large. This is to be expected because the illumination from the flame would obscure most droplets below the flame sheet. The resolution also limits the size of droplets that

can be discerned in this case. Figure 7 shows an example of the size of droplet commonly visible in this test.



Fig. 8: Progression of a roll wave in the liquid layer during the zoomed in test at atmospheric pressure. Droplets can clearly be seen escaping the wave and entraining in the flow in the second and third frames. The second frame is 0.013 seconds after the first and the third frame is another 0.004 seconds after that.

Zoomed-In View Atmospheric Test

This test captured more detail than the previous test because it only focuses on the front third of the fuel grain. The liquid layer instabilities can be clearly observed in the images. The parameters are very similar to the full view atmospheric run and can be found in Table 1.

The droplets visible in this test are much smaller than in the previous case. Figure 8 shows a roll wave developing in the liquid layer over several hundredths of a second. The vertical illumination on the left side of the image is the igniter wire burning. The wave grows, breaks up into droplets and entrains somewhat explosively into the flow. The number of droplets observed very near the fuel grain is much greater than the number of large drops viewed in the previous tests.

At the end of this test, localized reactions are visible at the fore end of the fuel grain. It is believed that these reactions occur through out the burn time, but can only be seen at the very end, when the mass flux is low. These reactions are shown in Figure 9.



Fig. 9: Flame bursting at the very end of the atmospheric pressure test of blackened paraffin.

III.II Elevated Pressure Test

The procedures for the elevated pressure test were nearly the same as in the atmospheric pressure tests. The main difference was that a graphite nozzle with a 1 cm diameter throat was installed. The expected pressure in the combustion chamber was determined by conducting cold flow tests and making allowance for a pressure increase due to combustion. Two high-speed video cameras were used to get both a full window view and a zoomed in view of each test. The fuel grain is shown in Figure 10.

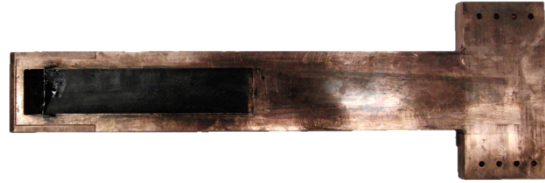


Fig. 10: The fuel grain for the elevated pressure test. This set up is the same as for the atmospheric pressure tests reported here.

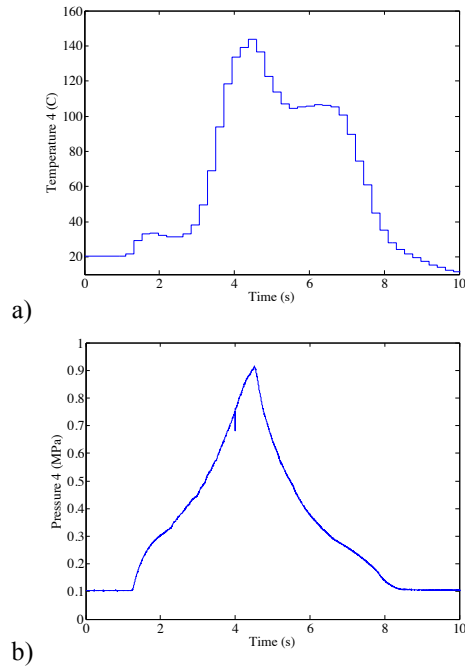


Fig. 11: a) Temperature and b) pressure data in the combustion chamber for the elevated pressure test.

This test was conducted at a low mass flux to keep the pressure at a manageable level. This test ran about one third of the amount of oxidizer through the system as the previous case. As previously described, cold flows were run to determine the pressure level for this run. However, the pressure rose dramatically beyond the designed level due to heating from the combustion process. The pressure curve from this test is shown in

Figure 11. It has an unusual shape due to the combustion heating. In most of the previous tests, the thermocouple in the combustion chamber (upstream of the fuel grain) was not exposed to temperatures above 20-30 C. However, in this case temperatures exceeded 100 C. All the images presented here are from about the first half of a second of the test, before the dramatic rise in temperature began to damage the windows and obscure the view.

The general progression of the flame is different from the atmospheric case. While the flame structure near the fuel grain and especially along the sides looks filament-like, the flow along the top of the grain has much more vertical movement than in the previous case, as can be seen in Figure 12. This may be caused by a combustion instability. It could also be the result of localized combustion reactions, like those observed at the end of the previous burn. Note that while the small illuminated circles in this image slightly resemble droplets, they are actually stationary reflections on the back window. Damage sustained to the window during the previous test causing these reflections to appear.

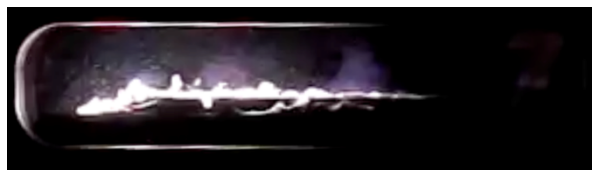


Fig. 12: Combustion at elevated pressure.

The structure of the flame is different than in the previous case. Roll waves cannot be made out in either of the views. The predominant features are elongated filaments. They run along the length of the fuel grain like streamers and can be seen in both Figures 12 and 13. It appears that at elevated pressures, the mass transfer mechanism changes.



Fig. 13: Filaments in the elevated pressure test of blackened paraffin.

The flame appears thicker than in the previous case because it extends both above and below the fuel grain. A composite image was constructed from the first 0.4 seconds of data. A frame was chosen every 0.025 seconds, they were placed on top of each other and made transparent to allow the brightest features to shine through. This composite image is shown in Figure 14. The composite image also gives insight into the structure of the flow. As was also apparent in Figure 12, the flame is much wavier than in the atmospheric case. Pulses of flame propagate with the flow.



Fig. 14: Thickness of the optically bright region of the flame from the elevated pressure test. The height of the red dots above the black baseline is given in millimeters.

IV. DISCUSSION

IV.1 Pressure Effects

The pressure in this test exceeded the supercritical limit for paraffin ($C_{32}H_{66}$), approximately 0.7 MPa.⁶ However, visual data was only available for the subcritical period of the test. Even the slight pressure elevation dramatically changed the behaviour of the combustion process. The liquid layer is much thinner in the elevated pressure case than at atmospheric pressure, as predicted.⁷ In the atmospheric case, it is quite easy to see the instabilities in the liquid layer. However the elevated pressure tests do not show this instability. It is likely that large-scale structure does not form because the liquid layer is so thin. Instead, ribbons of flame form along the length of the fuel grain. These typically extend below the level of the fuel grain. Structures resembling the flame bursting reactions observed at the end of the atmospheric test are visible throughout the elevated pressure test.

The ignition process occurs much faster in the elevated pressure case. While the flame takes a comparable amount of time to propagate down the length of the fuel grain, the initial flame is initially much larger than in the atmospheric case.

Damköhler Number

The Damköhler number (Da) is interesting in this case because it changes with pressure. It is given by the ratio of the characteristic fluid time to the characteristic chemical time. This value is typically assumed to be much greater than one for hybrid rockets, meaning that the chemical reactions do not limit the combustion process. However, because of the low mass flux, Da could actually be just a little greater than one for the atmospheric pressure runs of visualization experiment.

The characteristic fluid time scales as the ratio of the boundary layer thickness to the gas velocity in the combustion chamber ($\tau_f \sim \delta/U_\infty \sim 1/P$). As the pressure in this experiment is increased, the velocity in the combustion chamber will decrease. Therefore, the characteristic fluid time will increase.

The characteristic chemical time is also dependent on pressure. The reaction rate increases with increasing pressure. The characteristic chemical time is inversely

proportional to the reaction rate ($\tau_c \sim 1/RR$), which increases with pressure. Therefore, Da will tend to decrease with increasing pressure.

The combination of these pressure effects leads to an increase in Damköhler number with pressure. This is desirable because it can support the assumption that the process is not limited by chemical kinetics, even with the relatively low mass fluxes being used in this case.

IV.II Future Work

This area of research would further benefit from many additional tests at incremental pressures. This will allow the determination of the transition point between the behaviour observed at atmospheric pressure to that observed at higher pressure. It is also desirable to have optical observations at pressures above the supercritical limit for paraffin. The present system is capable of doing this by changing the oxidizer mass flux input into the system or swapping out the nozzle.

A more robust solution for the windows at elevated pressures is desired. While the polycarbonate windows provided a sufficient and inexpensive solution for the system at atmospheric pressure, they do not survive the higher heating levels for extended times at elevated pressure. The windows from the elevated pressure test reported here began sustaining damage after less than a second. Another option would be to reduce the burn

time at high pressures. However, such short burn times, like the one presented here could introduce biases caused by transient events.

V. CONCLUSIONS

The authors believe that the elevated pressure images presented here represent the first time hybrid combustion has been visualized with paraffin wax above atmospheric pressure. The goal of this experiment was to support improved combustion models and simulations of these fuels through observing entrained droplets and flame propagation. Combustion has been visualized at elevated pressures and compared to similar tests at atmospheric pressure.⁸ However, visualization at elevated pressures is more representative of the physical system.

There is a noticeable difference between the atmospheric and elevated pressure runs. Roll waves and droplets are clearly visible in the atmospheric test. However, these features are not apparent in the elevated pressure run. The predominant features in the elevated pressure run are elongated filaments running along the sides of the fuel grain. Additionally, upward bursts of flames can be seen in the elevated pressure run. This is believed to be caused by localized reactions occurring in regions with a combustible oxidizer to fuel ratio.

¹ Marxman, G. and Gilbert, M., *Turbulent Boundary Layer Combustion in the Hybrid Rocket*, Symposium (International) on Combustion, Vol. 9, 1963, pp. 371-383.

² Cantwell, B., Karabeyoglu, A., and Altman, D., *Recent Advances in Hybrid Propulsion*, International Journal of Energetic Materials and Chemical Propulsion, Vol. 9, No. 4, 2010, pp. 305-326.

³ Karabeyoglu, M. A., Cantwell, B. J. and Altman, D. *Development and Testing of Paraffin-Based Hybrid Rocket Fuels*. AIAA 2001-4503. 37th AIAA/ASME/SAE/ASEE Joint Propulsion Conference and Exhibit July 2001, Salt Lake City, Utah.

⁴ Mehta, R. D. and Bradshaw, P., *Design Rules for Small Low Speed Wind Tunnels*, Aero. Journal (Royal Aeronautical Society), Vol. 73, 1979, pp. 443.

⁵ Chandler, A. A. *An Investigation of Liquefying Hybrid Rocket Fuels with Applications to Solar System Exploration*. Ph.D. Thesis, Stanford University, 2012.

⁶ Karabeyoglu, M.A., Cantwell, B.J. and Stevens, J. *Evaluation of Homologous Series of Normal-Alkanes as Hybrid Rocket Fuels*. 41st AIAA/ASME/SAE/ASEE Joint Propulsion Conference & Exhibit. 10 - 13 July 2005, Tucson, Arizona. AIAA 2005-3908.

⁷ Karabeyoglu, M. A., Altman, D. and Cantwell B. J. *Combustion of Liquefying Hybrid Propellants: Part I, General Theory*. J. of Propulsion and Power, Vol. 18, No. 3, May-June 2002.

⁸ Nakagawa, I., Hikone, S. and Suzuki, T. *A Study on the Regression Rate of Paraffin-based Hybrid Rocket Fuels* 45th AIAA/ASME/SAE/ASEE Joint Propulsion Conference & Exhibit 2 - 5 August 2009, Denver, Colorado, USA. AIAA-2009-4935.